

## Angular dependence of the field-cooled, zero-field-cooled, and remanent magnetization in $\text{YBa}_2\text{Cu}_3\text{O}_7$ single crystal

U. Yaron and I. Felner

*Racah Institute of Physics, The Hebrew University, Jerusalem, 91904 Israel*

Y. Yeshurun

*Department of Physics, Bar-Ilan University, Ramat-Gan, Israel*

(Received 23 April 1991)

We have studied the angular dependence of the zero-field-cooled ( $M_{\text{ZFC}}$ ), field-cooled ( $M_{\text{FC}}$ ), and remanent magnetization ( $M_{\text{rem}}$ ) of  $\text{YBa}_2\text{Cu}_3\text{O}_7$  single crystal, by rotating the crystal relative to the applied field direction. The angular dependence of  $M_{\text{ZFC}}$  is governed only by the shape anisotropy of the crystal. Two mechanisms, namely, shape anisotropy and intrinsic anisotropy, are used to describe the angular dependence of the remanent magnetization. At sufficiently low fields and low temperatures,  $M_{\text{FC}}$  rotates with the crystal as a rigid entity, and the relation  $M_{\text{FC}} = M_{\text{ZFC}} + M_{\text{rem}}$  holds for all orientations. In the single crystal the measured and the calculated shape anisotropy ratios are equal, whereas for ceramic samples the calculated ratio is larger than the measured one.

### I. INTRODUCTION

Many recent investigations have probed the intrinsic anisotropy properties of the high- $T_c$   $\text{YBa}_2\text{Cu}_3\text{O}_7$  and Bi-Sr-Ca-Cu-O single crystals.<sup>1</sup> Lower<sup>2</sup> and upper<sup>3</sup> critical fields, London penetration depth,<sup>4</sup> and the critical current<sup>5</sup> density are only part of physical quantities which show intrinsic anisotropy. This anisotropy stems from the layered structure of Y-Ba-Cu-O and Bi-Sr-Ca-Cu-O, where superconductivity is confined to the Cu-O planes which are, in turn, coupled by the Josephson effect. Most studies of intrinsic anisotropy properties were restricted to directions along principal crystallographic axes and did not probe the full angular dependence of these quantities.

In earlier experiments<sup>6</sup> we demonstrated the existence of uniaxial anisotropy in Y-Ba-Cu-O and Bi-Sr-Ca-Cu-O crystals, by measuring the angular dependence of the remanent magnetization. In these experiments the crystals were cooled in an external field  $\mathbf{H}$  at different "cooling angles"  $\phi$ , where  $\phi$  is the angle between  $\mathbf{H}$  and the crystal  $c$  axis. At a temperature  $T < T_c$ , the field was turned off and the remanent magnetization  $M_{\text{rem}}$  was recorded while the crystals were rotated by an angle  $\theta$  relative to  $\mathbf{H}$ . The rotation angle is either in the Cu-O plane or perpendicular to it. The dominant feature of the measurements were the pronounced minima of  $M_{\text{rem}}$  at fixed angle  $\theta = 180^\circ$  independent of  $\phi$ , demonstrating the tendency to pin vortices in the  $c$  direction as predicted by models for anisotropic superconductors.<sup>7</sup> In similar measurements<sup>8</sup> on polycrystalline Y-Ba-Cu-O samples, we found these minima of  $M_{\text{rem}}$  to always be located at  $180^\circ$  relative to the cooling angle  $\phi$ , thus the external field  $\mathbf{H}$  defines an anisotropy direction.

The angular dependence of the magnetization moment of single crystals has recently been investigated by simultaneously measuring the longitudinal and transverse com-

ponents of the magnetization<sup>9</sup> for various orientations of the crystal with a respect to  $\mathbf{H}$ . These measurements, which were performed only at temperatures close to  $T_c$  and in relatively large fields, yield a value of 2.7 for the ratio between longitudinal and transverse magnetization. Similar measurements<sup>10</sup> on oriented grains of Y-Ba-Cu-O also show the anisotropy of the magnetization at different directions.

In the present paper we provide a detailed study of the angular dependence of the zero-field-cooled ( $M_{\text{ZFC}}$ ), field-cooled ( $M_{\text{FC}}$ ), and remanent ( $M_{\text{rem}}$ ) magnetization of the Y-Ba-Cu-O crystal at 4.2 K. We show that, in the low-field limit, when the pinning of vortices is sufficiently strong, the relation  $M_{\text{FC}} = M_{\text{ZFC}} + M_{\text{rem}}$  is valid in all orientations of the crystal relative to  $\mathbf{H}$ . For a higher applied field the pinning forces are weaker and we find that  $|M_{\text{FC}}| \leq |M_{\text{ZFC}} + M_{\text{rem}}|$ .

Magnetic measurements of crystals having a flat-plate geometry are governed by shape anisotropy since the effective demagnetization field seen by the sample is uniaxial. The magnetization values could be extremely difficult to handle properly as there is a severe competition between the intrinsic anisotropy mentioned above, and the shape anisotropy at different orientation. This problem will be discussed.

### II. EXPERIMENTAL DETAILS

The  $920 \times 410 \times 60 \mu\text{m}^3$  ( $a \times b \times c$ ), the Y-Ba-Cu-O crystal used in the present study was grown from a Y-Ba-Cu-O melt using the technique of Kaiser *et al.*<sup>11</sup> The crystal was subsequently annealed in flowing oxygen gas at  $450^\circ\text{C}$  for 14 days and was a single phase as judged by x-ray diffraction. The superconducting onset temperature of  $T_c = 92$  K was measured by ac susceptibility measurements. The width of transition in the ac measurements is of order 1 K.

Magnetic measurements reported here were carried out on a vibrating sample magnetometer (VSM) which enables a rotation of the sample relative to the external field. The experimental procedures are as follows. The sample was cooled to a low temperature either in a field (FC) ( $\phi$  is the cooling angle between  $\mathbf{H}$  and the  $c$  axis) or in nominal zero field (less than 3 Oe) (ZFC). In the ZFC measurements, the field was applied at 4.2 K and the sample was then rotated relative to  $\mathbf{H}$ . The axis of rotation was parallel to the  $a$ - $b$  plane. The moment was measured as a function of the angle  $\theta$  between  $\mathbf{H}$  and  $c$  and as a function of  $H$ . In the FC process, the sample was rotated in the cooling field and  $M_{FC}$  was measured as a function of  $\theta$ . In the remanent measurements, the sample was field cooled to low temperature. The field was then turned off and  $M_{rem}$  was measured as a function of  $\theta$ .

### III. EXPERIMENTAL RESULTS

#### A. Zero-field-cooled measurements

##### 1. Determination of the demagnetization factors

Figure 1 exhibits the low-field, ZFC magnetization curves of the Y-Ba-Cu-O crystal at various angles  $\theta$ . We recall that  $\theta$  is the angle between the external field  $\mathbf{H}$  and the crystallographic  $c$  axis and for the present experiment  $\theta = \phi$ . (The crystal is rotated around an axis in the  $a$ - $b$  plane which is parallel to  $a$ , the longest axis of the crystal.) It is readily seen that the curves are quite linear in this field range ( $H \leq 800$  Oe) which exceeds  $H_{c1}$ .<sup>12</sup> Small deviations from linearity above  $H_{c1}$  are also reported by other groups.<sup>10</sup> The slope of the magnetization  $-dM/dH$  decreases regularly with increasing  $\theta$  (i.e., the direction of  $\mathbf{H}$  is rotated away from the  $c$  direction). Assuming a perfect shielding for  $H < H_{c1}$ , we explain the decrease in  $M_{ZFC}$  for a given field by the variation of demagnetization factor  $N$  with  $\theta$ . The slopes of Fig. 1 can easily be described as

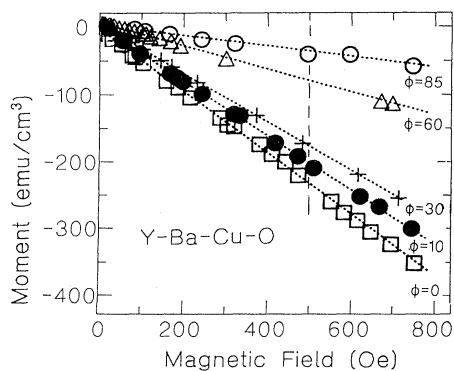


FIG. 1. Field dependence of the magnetization at low external fields at various orientations of the Y-Ba-Cu-O crystal ( $\theta = \phi$ ). The difference in the slopes are due to the angular dependence of the demagnetization factor.

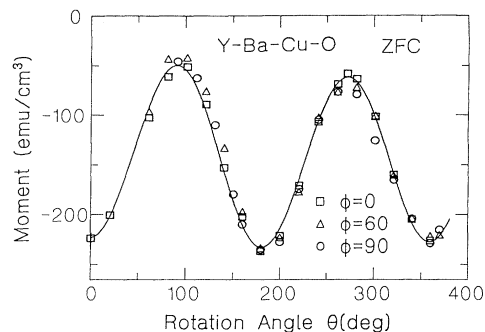


FIG. 2. Angular dependence of the zero-field-cooled magnetization for three different cooling angles at 4.2 K and  $H = 500$  Oe. Note the coincidence of the curves.

$$\frac{-dM}{dH} = A \cos^2\theta + B \sin^2\theta, \quad (1)$$

where  $A = 1/4\pi(1 - N_c)$  and  $B = 1/4\pi(1 - N_b)$ , and  $N_{b,c}$  are the demagnetization correction factors parallel to  $b$  and  $c$ . Justification for Eq. (1) will be given in a later paragraph.

From the different slopes of the curves, we could extract the demagnetization correction factors of the crystal at various orientations. The values of the demagnetization factors  $N_b = 0.84$  and  $N_c = 0.13$  (parallel to  $b$  and  $c$ , respectively) are in excellent agreement with values calculated by approximating the crystal as an ellipsoid of rotation and using conventional tables.<sup>13</sup>

##### 2. Angular dependence of $M_{ZFC}$

We start with the results of measurements of  $M_{ZFC}$  at 500 Oe and 4.2 K for rotating the Y-Ba-Cu-O crystal around an axis parallel to  $a$ . Figure 2 exhibits the angular dependence of  $M_{ZFC}$  as a function of  $\theta$  for three different cooling angles. It is apparent that all the curves are totally independent of  $\phi$ . On the time scale of the experiment ( $\sim 5$  min), the data presented in Fig. 2 are “re-

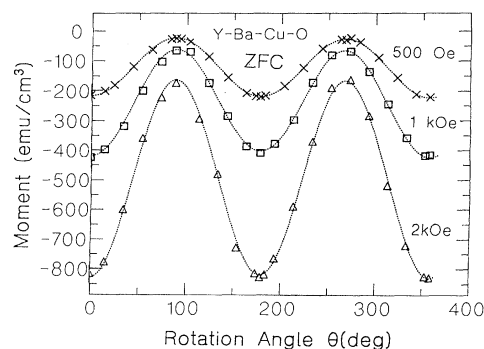


FIG. 3. Angular dependence of the zero-field magnetization of the Y-Ba-Cu-O crystal at 4.2 K and various applied fields.

versible," namely, that by reversing the sense of rotation, we trace back the original values. The solid line in Fig. 2 is fit to<sup>14</sup>

$$-M_{ZFC} = -H(A \cos^2\theta + B \sin^2\theta). \quad (2)$$

We show below that the physics which leads to Eq. (2) is identical to that which leads to Eq. (1). We also note that the curves in Fig. 2 just trace the vertical line in Fig. 1.

To obtain Eqs. (1) and (2) we have to define  $M_b$  and  $M_c$ ,  $N_b$  and  $N_c$  as the magnetization and demagnetization factors, respectively, along the principal axes of the crystal. As mentioned earlier, the deviation from linearity of the  $M$  versus  $H$  curves at 500 Oe for all  $\phi$  is negligible (Fig. 1). Assuming complete exclusion of flux, the susceptibility tensor is diagonal with  $-1/4\pi$  elements, and the magnetizations obtained are

$$M_b = -H \sin\theta / 4\pi(1 - N_b)$$

and

$$M_c = -H \cos\theta / 4\pi(1 - N_c),$$

where  $H$  is the external field.

Recalling that the VSM measures only the component of  $M$  along the direction of  $H$ , we get

$$M_{ZFC}(\theta) = M_c \cos\theta + M_b \sin\theta \\ = -H[\cos^2\theta / 4\pi(1 - N_c) + \sin^2\theta / 4\pi(1 - N_b)],$$

which is exactly the form of Eqs. (1) and (2).

So far we have discussed data of  $M_{ZFC}$  at 4.2 K and for  $H=500$  Oe. In Fig. 3 we present  $M_{ZFC}(\theta)$  data for  $H=1$  and 2 kOe, and, for the sake of comparison, the curve for 500 Oe is also shown. We note the similarity among the curves all of which are fitted to Eq. (2) (dotted lines in the figure). The main effect of the increase in the field is to reduce the coefficients  $A$  and  $B$ , reflecting the reduction of the susceptibility to a value smaller than  $-1/4\pi$ .

### B. Remanent measurements

Figure 4 shows the angular dependence of the remanent magnetization for various  $\phi$  cooling angles. Similar results have been thoroughly dealt with and ex-

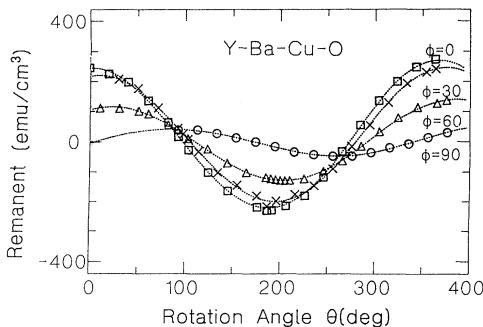


FIG. 4. Angular dependence of the remanent magnetization for the indicated cooling angles at 4.2 K and a cooling field of 500 Oe of the Y-Ba-Cu-O crystal.

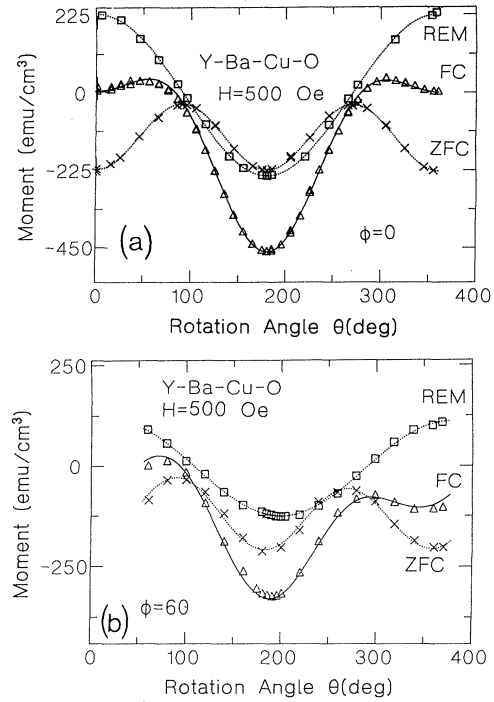


FIG. 5. Angular dependence of the remanent, zero-field-cooled, and field-cooled magnetizations for the Y-Ba-Cu-O crystal at 4.2 K and a cooling field of 500 Oe for the cooling angle (a)  $\phi=0$  and (b)  $\phi=60$ . Solid lines are fitted to Eq. (4).

plained in a previous paper.<sup>6</sup> However, the measurements reported here were performed on another crystal and the interpretation of the data given here is slightly different, as explained below.

In Fig. 4 the crystal is cooled to 4.2 K in 500 Oe at various cooling angle of  $\phi$ . The remanent magnetization is obtained when the field is turned off and the angular dependence data, obtained during the rotation of the crystal to  $\theta=360$  and backwards to  $\theta=0^\circ$  in zero field, fit nicely to

$$M_{\text{rem}}(\theta, \phi) = M_{\text{rem}}^c \cos\theta \cos\phi + M_{\text{rem}}^{ab} \sin\theta \sin\phi, \quad (3)$$

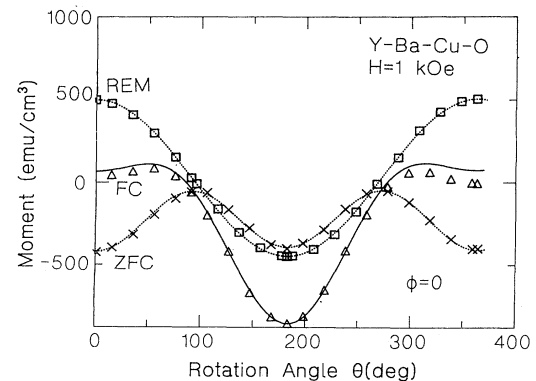


FIG. 6. (a) Angular dependence of  $M_{\text{rem}}$ ,  $M_{\text{FC}}$ , and  $M_{\text{ZFC}}$  at 4.2 K for the cooling field 1000 Oe. The solid line is the sum of  $M_{\text{ZFC}} + M_{\text{rem}}$ . Note that  $|M_{\text{FC}}| \leq |M_{\text{ZFC}} + M_{\text{rem}}|$ .

where  $M_{\text{rem}}^c$  and  $M_{\text{rem}}^{ab}$  are the remanent values measured for  $\phi=0$  at  $\theta=0$  ( $\mathbf{H}\parallel\mathbf{c}$ ) and for  $\phi=90^\circ$  at  $\theta=90^\circ$  ( $\mathbf{H}\perp\mathbf{c}$ ), respectively.

The dominant features in these curves are the pronounced minima at angles close to  $\theta=180^\circ$  independent of the initial cooling angle  $\phi$  (except for  $\phi=90^\circ$  where the minimum is shifted towards  $270^\circ$ ). To understand these observations we recall again that, in a VSM, the measured magnetization is only the component of  $\mathbf{M}$  along the magnetic field. When during the cooling process  $\mathbf{H}$  is in the direction of  $\mathbf{c}$  or  $\mathbf{a}$  ( $\phi=0$  or  $\phi=90^\circ$ ), the vortex lines are aligned parallel to the magnetic field and are trapped and pinned in that direction. The obtained remanents are  $M_{\text{rem}}^c$  or  $M_{\text{rem}}^{ab}$  and upon rotation we measure their components along the field direction  $M_{\text{rem}}^c \cos\theta$  or  $M_{\text{rem}}^{ab} \sin\theta$ . Since the initial values of the remanent depends on the initial conditions,<sup>6</sup> namely, on the angle  $\phi$  between  $\mathbf{H}$  and  $\mathbf{c}$  during the cooling process, the data of Fig. 4 fit nicely to the superposition of the two terms of Eq. (3).

Trapping is extremely anisotropic. We obtain for the present crystal the anisotropy ratio  $M_{\text{rem}}^c/M_{\text{rem}}^{ab} \approx 5$ . Thus, when the field is turned off, the first term in Eq. (3) is the dominant one, and the location of the minima in Fig. 4 are close to  $\theta=180^\circ$ . It should be added that, in a previous paper,<sup>6</sup> we assigned a constant instead of the second term of Eq. (3). We then realized that this constant is related to flux trapped in the  $a$ - $b$  plane but could not extract its angular dependence because of the ex-

tremely large anisotropy ratios (7 for Y-Ba-Cu-O and 50 for Bi-Sr-Ca-Cu-O).

### C. Field-cooled measurement

To complete the experimental description, we measured the angular dependence of the field-cooled magnetization  $M_{\text{FC}}$  at various cooling angles  $\phi$  and different applied fields  $H$ . Figure 5a illustrates the  $M_{\text{FC}}$  data (triangles) as a function of  $\theta$  for  $\phi=0$  and  $H=500$  Oe. For the sake of comparison, the  $M_{\text{ZFC}}$  and  $M_{\text{rem}}$  measured under these conditions are also shown. All the curves in this figure represent data obtained when the crystal was rotated from  $\theta=0$  to  $\theta=360$  and backward. Figure 5(b) shows the same curves obtained at  $\phi=60^\circ$ . The most striking feature in these figures is the fact that  $M_{\text{FC}}$  is the sum of the two other curves. Indeed, the solid lines in both Figs. 5(a) and 5(b) describe the results of a least-squares fit to

$$M_{\text{FC}} = A \cos^2\theta + B \sin^2\theta + M_{\text{rem}}^c \cos\theta \cos\phi + M_{\text{rem}}^{ab} \sin\theta \sin\phi, \quad (4)$$

which is the sum of Eqs. (2) and (3). This fit yields the same parameters which were obtained previously for each of the curves. Thus, the relation  $M_{\text{FC}} = M_{\text{ZFC}} + M_{\text{rem}}$  is valid for all orientations of the crystal. This implies that the magnetization is fixed in the crystal frame of reference and rotates with the crystal. In other words, the Lorentz force is not strong enough to result in a lag angle between  $M_{\text{FC}}$  and the external field.

On the other hand, for higher external fields at 4.2 K,  $|M_{\text{FC}}| \leq |M_{\text{ZFC}} + M_{\text{rem}}|$ . The triangles in Fig. 6 represent the angular dependence of  $M_{\text{FC}}$  at  $H=1$  kOe and the solid line is again the calculated values of  $M_{\text{ZFC}} + M_{\text{rem}}$  at 1 kOe. The inequality is quite evident, in particular around  $0^\circ$  and  $360^\circ$ . Moreover, the low- $\theta$  region of Fig. 7(a) demonstrates that at 2 kOe the backward  $M_{\text{FC}}(\theta)$  differs significantly from the forward curve. This is, in fact, even more dramatic for  $H=10$  kOe. Figure 7(b) shows the angular dependence of the remanent, the zero-

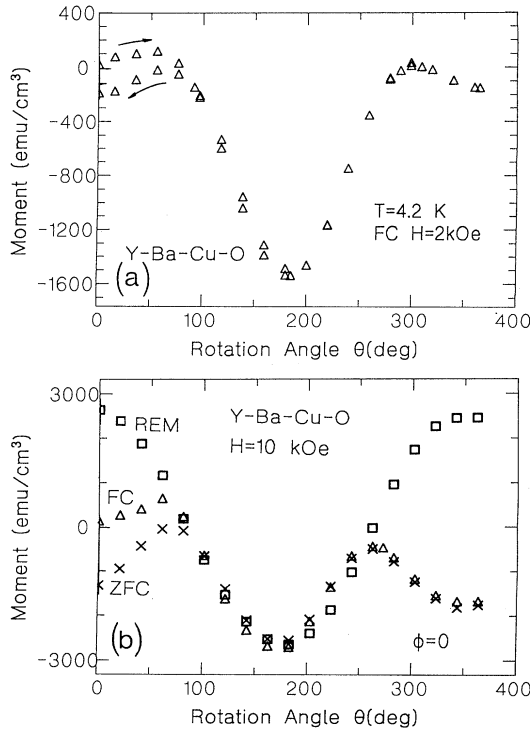


FIG. 7. (a) Angular dependence of  $M_{\text{FC}}$  for the cooling field 2 kOe and cooling angle  $\phi=0$  at 4.2 K. Arrows indicate the direction of the rotation. (b) Angular dependence of  $M_{\text{FC}}$ ,  $M_{\text{ZFC}}$ , and  $M_{\text{rem}}$  at 4.2 K for a cooling field of 10 kOe ( $\phi=0$ ). Note the break of  $M_{\text{FC}}$ .

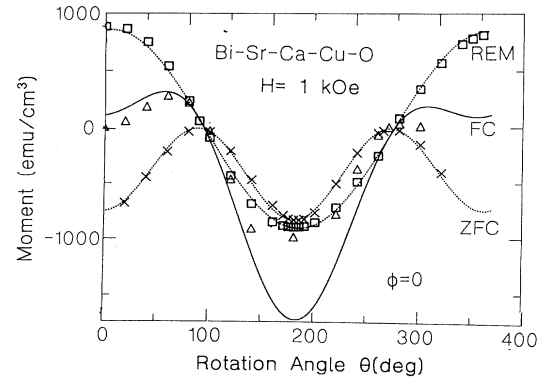


FIG. 8. Angular dependence of  $M_{\text{FC}}$ ,  $M_{\text{ZFC}}$ , and  $M_{\text{rem}}$  for the Bi-Sr-Ca-Cu-O crystal at 4.2 K for a cooling field of 1 kOe. Note the break of  $M_{\text{FC}}$ . The solid line is the sum of the  $M_{\text{ZFC}}$  and  $M_{\text{rem}}$  curves [Eq. (4)].

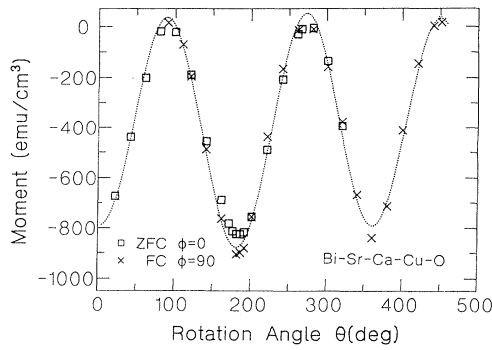


FIG. 9. Angular dependence of  $M_{ZFC}$  at  $\phi=0$  and  $M_{FC}$  at  $\phi=90$  for the cooling field 1 kOe at 4.2 K for the Bi-Sr-Ca-Cu-O crystal.

field magnetization, and the field-cooled magnetization at 4.2 K for  $H = 10$  kOe. It is quite obvious that, in the FC process, there is a total breaking of the rigid moment and the  $M_{FC}$  curve collapses toward the  $M_{ZFC}$  curve.

For the sake of comparison, the magnetization data for Bi-Sr-Ca-Cu-O crystal are shown in Fig. 8 (it is the same crystal studied in Ref. 6). The figure shows the angular dependence of  $M_{FC}$ ,  $M_{ZFC}$ , and  $M_{rem}$  at 4.2 K for  $H = 1$  kOe. In contrast to Fig. 6, in this case the field-cooled magnetization is completely destroyed and coincides with the  $M_{ZFC}$  curve in most of the angular regime. The solid line represents  $M_{ZFC} + M_{rem}$  and the huge differences between this curve and  $M_{FC}$  are evident.

It appears that in Y-Ba-Cu-O in the presence of a high external field, the direction of the vortices could be very different from the original trapped direction. The field exercises a force on the flux lines and by rotation they are driven out of the sample. The pinning forces for the Bi-Sr-Ca-Cu-O crystal are weaker than for the Y-Ba-Cu-O crystal and under the same field and temperature conditions  $M_{FC}$  is completely collapsed. It should also be noted that several Y-Ba-Cu-O crystals measured by us have shown the same tendency of  $M_{FC}$  to coincide with the  $M_{ZFC}$  curve at relatively low applied fields. The present Y-Ba-Cu-O crystal, for which we show data here, exhibits stronger pinning forces. As a final point of interest, it is worth showing that, for Bi-Sr-Ca-Cu-O crystal, the  $M_{ZFC}$  curve coincides with the  $M_{FC}$  curve obtained for  $\phi=90^\circ$ , Fig. 9. This overlap is due to the extremely small flux trapping in the  $a$ - $b$  plane of this sample.<sup>6</sup>

#### IV. DISCUSSION

It is quite clear that anisotropy governs our experimental results. In a previous paper,<sup>6</sup> which dealt with remanent magnetization results, we suggested a simple scenario for the organization of the vortex lines. According to this scenario, based on models for anisotropic superconductors,<sup>7</sup> flux lines tend to align themselves along the  $c$  axis of the unit cell. This anisotropy is consistent, at least qualitatively, with the measured anisotropy of the critical current  $J_c$ ,<sup>5</sup> since preferred flux trapping along the  $c$  axis is equivalent to larger  $J_c$  in the  $a$ - $b$  plane.

Kolensik *et al.*,<sup>15</sup> however, argued that the observed anisotropy results mainly from the shape of the sample and is not intrinsic. They based their claim on the observation of similar anisotropy in a thin disc of polycrystalline Nb foil. As mentioned above, in our crystal both the shape anisotropy ratio  $(1-N_b)/(1-N_c)$  and the measured  $M_{rem}^c/M_{rem}^{ab}$  are equal to 5. It is possible, then, that the angular dependence of the remanent magnetization does not reflect the intrinsic anisotropy of magnetic flux trapping, but rather reflects the strong angular dependence of the demagnetization factor. Taking into account the relation  $H_{in} = H/(1-N)$ , where  $H_{in}$  and  $H$  are the internal and the external fields respectively, the large  $N_c$  gives rise to large internal field during the cooling process which causes large flux trapping when  $\mathbf{H} \parallel \mathbf{c}$ .<sup>16</sup>

These two competing explanations led us to carry out a few other experiments on the present crystal and on polycrystalline Y-Ba-Cu-O samples. Figure 10 shows the initial values of the remanent moments,  $M_{rem}^c(\mathbf{H} \parallel \mathbf{c})$  and  $M_{rem}^{ab}(\mathbf{H} \parallel \mathbf{ab})$  of the Y-Ba-Cu-O crystal at 4.2 K as a function of the applied cooling field. This figure also shows the anisotropy ratio  $M_{rem}^c/M_{rem}^{ab}$  as a function of the applied cooling field. Unfortunately, a small piece of the crystal was broken just before these measurements and the anisotropy ratio after cooling at 500 Oe is slightly smaller than that reported earlier in this paper. The fact that a change of dimensions causes a change in the anisotropy ratio points to the importance of the shape in determining this ratio. On the other hand, in the high-field regime, the demagnetization effect is weak and the difference between  $H$  and  $H_{in}$  is small. The anisotropy ratio (Fig. 10), however, is essentially constant and hardly depends on the applied field value. This result implies that the origin of anisotropy is intrinsic and not an artifact of the shape of the crystal. The two observations just mentioned are contradictory, a fact which interferes with our ability to reach a decisive conclusion.

We have also performed some more measurements on polycrystalline samples. Figure 11 shows the angular dependence of  $M_{rem}$  after field cooling at 500 Oe of a flat polycrystalline Y-Ba-Cu-O sample ( $2.1 \times 1.7 \times 0.15$  mm<sup>3</sup>)

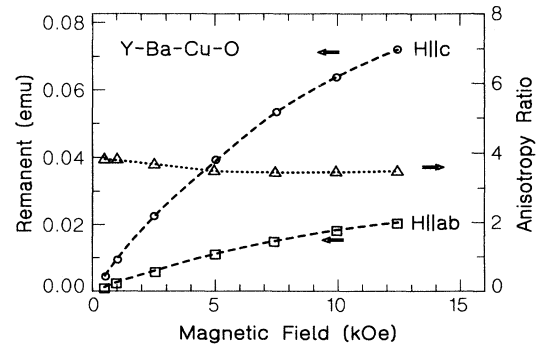


FIG. 10. Dependence of the remanent magnetization on the cooling field for  $\mathbf{H} \parallel \mathbf{c}$  and  $\mathbf{H} \parallel \mathbf{ab}$  planes of the Y-Ba-Cu-O crystal, and the field dependence of the anisotropy ratio  $M_{rem}^c/M_{rem}^{ab}$ . Note that the anisotropy ratio is essentially independent of the cooling field.

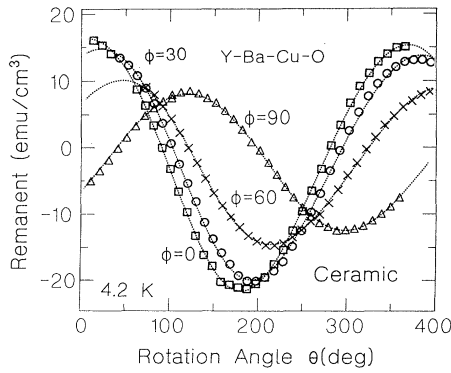


FIG. 11. Angular dependence of the remanent magnetization for the indicated cooling angles  $\phi$  at 4.2 K and cooling field of 500 Oe for a flat ceramic Y-Ba-Cu-O sample.  $\phi=0$  for  $\mathbf{H}$  parallel to the thin dimension.

at different cooling angles  $\phi$ . This measurement was followed by a series of similar measurements performed on three disc-shaped ceramic Y-Ba-Cu-O samples of different thicknesses. All the ceramic samples were characterized by x-ray diffraction and were found to be granular with no preferred orientation. The shape anisotropy ratio was obtained by measuring  $M$  versus  $H$  after a ZFC process, and from our remanent measurements by three alternative ways: (a) a direct measurement of the initial remanent values at  $\theta=\phi=0$  and  $\theta=\phi=90$  ( $\phi=0$  for  $\mathbf{H}$  parallel to the thin dimension), (b) a fit of the angular dependence of  $M_{\text{rem}}$  to Eq. (3), and (c) by observing the location of the minima of the  $M_{\text{rem}}$  curves. The location of the minima  $\theta_{\text{min}}$  could be related to the anisotropy ratio by a differentiation of Eq. (3) with respect to  $\theta$  which yields

$$M_{\text{rem}}^c / M_{\text{rem}}^{ab} = \tan\phi / \tan\theta_{\text{min}} \quad (\phi \neq 0, 90). \quad (5)$$

The anisotropy ratio extracted from the  $M$  versus  $H$  measurements and from the first two remanent methods were similar. The ratio extracted by the last method was field dependent, and was larger for smaller fields. However, all the measured ratios were significantly smaller than the

calculated ratios (based on the approximation to an ellipsoid<sup>13</sup> and assuming that the demagnetization factor of a highly compact specimen is imposed by its macroscopic shape<sup>14</sup>). The disagreement between the calculated and the measured ratios of all polycrystalline samples is in a qualitative agreement with Ref. 17, which claims that the ellipsoid approximation applied to the thin discs leads to anisotropy ratios which are larger than the experimental ones. This result is in contrast to the similarity of the calculated and experimental ratios obtained for our single crystal. The anisotropy ratios measured by ZFC and remanent processes are similar for both polycrystalline samples and the single crystal. Furthermore, the anisotropy observed in the ZFC and remanent measurements of the polycrystalline samples and in the ZFC measurements of the single crystal is induced only by the shape of the sample. Both facts combined together point to the importance of the shape in determining the anisotropy ratio in remanent measurements of single crystals.

## V. CONCLUSION

The experimental results reported in this paper and the proposed analysis strongly suggest that the angular dependence of the zero-field magnetization is governed only by the shape anisotropy of the crystal. The angular dependence of the remanent can be interpreted using two compatible mechanisms, namely, the intrinsic anisotropy or the shape anisotropy, and the present study cannot support either one of them. For low external fields the field-cooled moment rotates with the crystal as a rigid entity and the relation  $M_{\text{FC}} = M_{\text{ZFC}} + M_{\text{rem}}$  holds for all orientation of the crystal. For higher fields the  $M_{\text{FC}}$  is irreversible and flux lines are driven out of the sample. For the single crystal the measured and the calculated shape anisotropy ratios are equal, in sharp contrast to ceramic materials where the calculated ratios exceed the measured values.

## ACKNOWLEDGEMENTS

This research was supported by a grant from the Ministry of Science and Technology of the State of Israel and by the Klachky Foundation for Superconductivity.

<sup>1</sup>D. E. Farrell *et al.*, Phys. Rev. Lett. **63**, 782 (1989).  
<sup>2</sup>L. Krusin-Elbaum, A. P. Malozemoff, Y. Yeshurun, D. C. Cronemeyer, and F. Holtzberg, Phys. Rev. B **39**, 2936 (1989); T. R. Dinger *et al.* Phys. Rev. Lett. **58**, 2687 (1987).  
<sup>3</sup>U. Welp, W. K. Kwok, G. W. Crabtree, K. G. Vandervoort, and J. Z. Liu, Phys. Rev. Lett. **62**, 1908 (1989).  
<sup>4</sup>L. Krusin-Elbaum, R. L. Greene, F. Holtzberg, A. P. Malozemoff, and Y. Yeshurun, Phys. Rev. Lett. **62**, 217 (1989).  
<sup>5</sup>Y. Enomoto, T. Murakami, M. Suzuki, and K. Moraka, J. Appl. Phys. **26**, L1248 (1987).  
<sup>6</sup>I. Felner, U. Yaron, Y. Yeshurun, G. V. Chandrashekar, and F. Holtzberg, Phys. Rev. B **40**, 5239 (1989).  
<sup>7</sup>V. G. Kogan, Phys. Rev. B **38**, 7049 (1988).  
<sup>8</sup>Y. Wolfus, Y. Yeshurun, and I. Felner, Phys. Rev. B **37**, 3667

(1988).  
<sup>9</sup>M. Tuominen, A. M. Goldman, Y. Z. Chang, and P. Z. Jiang, Phys. Rev. B **42**, 412 (1990).  
<sup>10</sup>S. Senoussi and C. Aguilon, Europhys. Lett. **12**, 273 (1990).  
<sup>11</sup>D. L. Kaiser, F. H. Holtzberg, M. F. Chisholm, and T. K. Worthington, J. Cryst. Growth **85**, 593 (1987).  
<sup>12</sup>M. McElfresh, *et al.*, Physica A **168**, 308 (1990).  
<sup>13</sup>J. A. Osborn, Phys. Rev. **67**, 351 (1945).  
<sup>14</sup>S. Senoussi, S. Hadjoudj, R. Maury, and A. Fert, Physica C **165**, 364 (1990).  
<sup>15</sup>S. Kolesnik, T. Skoskiewicz, and J. Igalson, Phys. Rev. B **43**, 13 679 (1991).  
<sup>16</sup>A. P. Malozemoff *et al.*, Phys. Rev. B **38**, 6490 (1988).  
<sup>17</sup>M. N. Kunchur and S. J. Poon, Phys. Rev. B **43**, 2916 (1991).